In silico studies on pyrazine derivatives for identifying potential inhibitors of PIM-1 kinase

Amena Ali[1], Abuzer Ali[1], Mohd. Washid Khan[2], Abutahir[3], Ibraheem Husain[4], Kuldeep Patel[5], Vivek Asati[5*]

[1]College of Pharmacy, Taif University, Taif, Saudi Arabia.
[2]Department of P.G. Studies and Research in Chemistry and Pharmacy, Rani Durgavati University, Jabalpur, India.
[3]Department of Pharmacology, Raghukul College of Pharmacy, Bhopal, India.
[4]Department of Pharmacology, MESCO Institute of Pharmacy, Amroha, India.
[5]Department of Pharmaceutical Chemistry, NRI Institute of Pharmaceutical Sciences, Bhopal, India.

ARTICLE INFO

ABSTRACT

PIM-1 kinase (PIM-1K) modulates multiple cellular functions and is evolving as a drug target for cancer. In search of potential PIM-1 inhibitors, we report herein the 3D-QSAR as well as docking studies on 3-(pyrazin-2-yl)-1H-indazole derivatives. Based on the 3D-QSAR study, the generated pharmacophore was utilized for the virtual screening of thousands of compounds (compds) from ZINC database against PIM-1K. Four top-ranked compds, ZINC05885218, ZINC05888770, ZINC08652441, and ZINC73096248, were selected by virtual screening study. The study results of molecular docking suggested that certain key residues were significant for interactions of ligand–receptor due to the formation of hydrogen bonds with Glu171, Glu121, Lys67, Asp128, Asp131 and Asp186 of PIM-1K. Virtually screened compds displayed resemblance in binding interactions within the PIM-1Ks catalytic pocket in comparison with their corresponding crystal structures. The ADRRR.2 emerged as the potential pharmacophore hypothesis and was employed for the generation of model of 3D-QSAR which gave good statistical values of q^2 and r^2 using partial least square analyses ($r^2 = 0.922$, $q^2 = 0.8629$) for the best model. The study results revealed that ZINC73096248 could serve as a prototype compd for developing novel PIM-1K inhibitors.

INTRODUCTION

PIM kinases (PIM-Ks) are significant serine/threonine kinases which are widely used in cellular transcription as well as translation (Cuypers *et al*., 1984). They occur generally in three distinct isoforms: PIM-1 kinase (PIM-1K), PIM-2K, and PIM-3K. These isoforms have similar functions and are involved in cell processes like multiplication, differentiation, and apoptosis (Fox *et al*., 2003). These PIM-Ks show weak oncogenic activity in their transgenic forms but exhibit increased activity when expressed along with c-Myc, a transcription factor (Forshell *et al*., 2011; Zhang *et al*., 2008). Alteration in the PIM-K pathway is associated with hematological malignancies or solid tumors (Brault *et al*.,

2010). Interestingly, PIM-1 and 2 are progressively expressed in multiple myeloma, lymphomas, and leukemia, whereas PIM-3 is predominantly predicted in the tumors of colon, pancreas, prostate, and some other organelles (Nawijn *et al*., 2011). Moreover, the deficiency of PIM-1K leads to failure in cell growth and survival. Nevertheless, PIM-1K is linked to drug resistance and is associated with cancer metastasis, immunotherapy, and epigenetic dynamics (Tursynbay *et al*., 2016). Consequently, PIM-Ks are promising therapeutic targets in drug development for cancer treatment (Asati *et al*., 2014). The *in vivo* study on mice proved that the inhibition of these kinases produced minimum side effects (Mikkers *et al*., 2004). Different inhibitors of PIM-K, for example, SGI-1776, AZD1208, and SMI-4a, were studied against chronic lymphocytic leukemia cells, solid and hematological cancers. However, AZD1208 is under clinical trials (Cervantes-Gomez, *et al*., 2016; Cortes *et al*., 2018). In one study carried out, Wang *et al*. (2015) reported 3-(pyrazin-2-yl)-1H-indazole derivatives as potential PIM-K inhibitors. Furthermore, Xu *et al*.

Corresponding Author
Vivek Asati, Department of Pharmaceutical Chemistry, NRI Institute of Pharmaceutical Sciences, Bhopal, India.
E-mail: vivekasatipharma47 @ gmail.com

(2014) have synthesized pyrazolo[1,5-a]pyrimidine derivatives as selective inhibitors of PIM-1K. Keeping the above-mentioned facts in mind, the present study was carried out on a series of pyrazine-linked indazoles to discover the structural requirements as potent PIM-1 inhibitors.

MATERIAL AND METHODS

Data set and Pharmacophore modeling

A data set of 29 compds belonging to 3-(pyrazin-2-yl)-1H-indazoles as inhibitors of PIM-1K were taken for pharmacophore generation, 3D-QSAR, and docking performances. The chemical structures of the above-mentioned series were selected from reported literature (Wang *et al.*, 2015). Different pharmacophore hypotheses were created by using this series, which were subsequently utilized for the 3D-QSAR model creation. The training and test set molecules general selection are given in Table 1. The 3D-QSAR model generation and pharmacophore modeling were carried out by utilizing PHASE module of Schrodinger (Dixon *et al.*, 2006).

Ligand preparation

In this module, prepared structures of compds were used and processed for wizard (Ligprep, version 2.5, Schrodinger, NY, 2012). The activity of all molecules was added manually with their pIC_{50} values. 2D structures were converted into 3D structures through cleanup wizard (Watts *et al.*, 2010). The alignment of all the 29 ligands are shown in Figure 1a. Subsequently, conformer generation was carried out by ConfGen macromodel search method with the application of OPLS-2005 force field (Schrodinger, LLC, 2015). All the molecules were distributed into a training set comprising 24 molecules and a test set of 5 molecules through leave-one-out process. The validation of created models was carried out by utilizing test set. A random activity threshold value was given to split training set molecules into 12 actives ($pIC_{50} >$ 8.6), 11 intermediates ($8 < pIC_{50} < 8.6$), and 6 inactives ($pIC_{50} < 8$).

Pharmacophore sites Creation and Score hypothesis

The pharmacophoric features were defined by specific SMARTS patterns and common pharmacophores were examined from 12 actives (4.4 version of PHASE, Schrodinger, 2012).

Table 1. Experimental and predicted activity data for training and test set compds (PLS factors = 5).

Compd QSAR set Experimental	Activity (pIC_{50})	Predicted activity	(pIC_{50})	Pharm set
1	TR	7.3	6.896	INACT
2	TR	8.5	8.523	Intermediate
3	TR	8.58	8.699	ACT
4	TR	7.9	7.959	INACT
5	TR	7.85	7.959	INACT
6	TR	8.17	8.155	Intermediate
7	TR	7.19	7.357	INACT
8	TR	8.99	8.699	ACT
9	TE	8.58	8.699	ACT
10	TR	8.6	8.523	Intermediate
11	TE	7.9	7.824	INACT
12	TR	8.07	8.097	Intermediate
13	TE	8.55	8.155	Intermediate
14	TR	8.53	8.523	Intermediate
15	TR	9.05	9.398	ACT
16	TR	8.86	8.523	Intermediate
17	TR	9.08	9.046	ACT
18	TR	8.87	8.796	ACT
19	TE	8.3	8.398	Intermediate
20	TR	8.54	8.699	ACT
21	TR	8.55	8.398	Intermediate
22	TR	8.42	8.523	Intermediate
23	TR	7.72	7.824	INACT
24	TR	8.33	8.523	Intermediate
25	TR	9.5	9.699	ACT
26	TR	9.41	9.398	ACT
27	TR	9.3	9.301	ACT
28	TR	9.06	8.854	ACT
29	TE	9.32	9.523	ACT

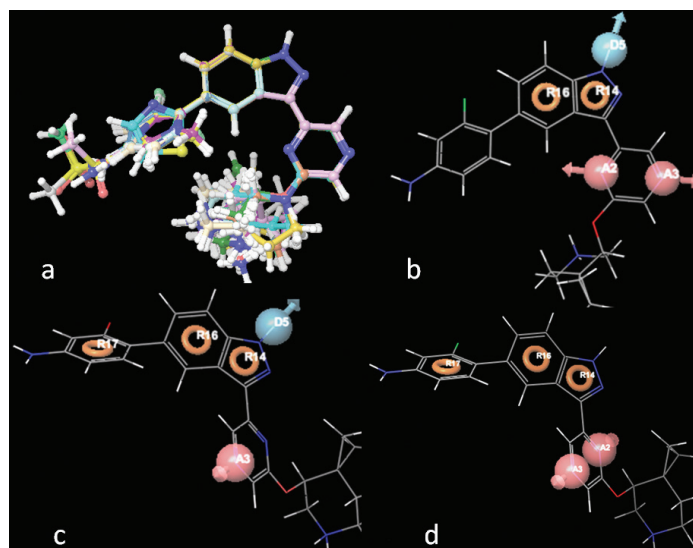TR = Training; TE = Test; INACT = Inactive; ACT = Active.

Figure 1. (a) Alignment of 29 molecules of 3-(pyrazin-2-yl)-1H-indazole derivatives; (b) compd 25 aligned with AADRR; (c) ADRRR; and (d) AARRR.

Table 2. Various hypotheses created by PHASE/scoring results.

S. No.	CPHs	Survival	Survival-inactive	Site	Vector	Volume	Matches
1	AADRR.8	3.852	1.039	1	1	0.857	1.439
2	ADRRR.2	3.829	1.03	0.99	0.995	0.839	1.64
3	ADRRR.15	3.819	1.02	0.99	0.983	0.841	1.645
4	ADRRR.62	3.818	1.02	0.99	0.983	0.841	1.687
5	AARRR.2	3.817	1.023	0.99	0.983	0.842	1.562
6	AADRR.69	3.785	0.991	0.98	0.953	0.853	1.467

Hypotheses were grouped based on the resemblance in identical and variant scores (Table 2). The actives with acceptable fitness scores were carefully chosen and further employed for the 3D-QSAR model creation (Kamaria and Kawathekar, 2014; Sallam *et al.*, 2013).

3D-QSAR data setting

On the basis of aligned ligands of selected hypothesis, the 3D-QSAR models were generated. In the following study, a total of six pharmacophore models were carefully chosen for the final 3D-QSAR models development (Golbraikh and Tropsha, 2002; Lather *et al.*, 2008). These 3D-QSAR models help in elucidation of SAR of all compds (Shah *et al.*, 2010).

Virtual screening

The pharmacophore (ADRRR) used for study and different libraries, like NCI (National Cancer Institute) and ZINC (2.5 million commercially available compds), were used for the virtual screening studies (Irwin and Shoichet, 2005). Lipinski rules of five were applied to choose the drug like compds to develop the potential inhibitors (Lipinski *et al.*, 2001).

Molecular docking

Docking studies on binding site of PIM-1K for 3-(pyrazin-2-yl)-1H-indazoles were accomplished by Glide v3.8 module of Schrodinger, NY (Friesner *et al.*, 2004, 2006; Halgren

et al., 2004; Sliwoski *et al.*, 2014). Protein data bank was used to obtain the PIM-1Ks (PDB ID: 2XJ1) crystal structure (Protein preparation wizard Schrodinger, 2012). Another comparative study of 3-(pyrazin-2-yl)-1H-indazoles was carried out on PIM-1Ks crystal structure by Autodock Vina module (Seeliger and Groot, 2010).

MM/GBSA-based rescoring and enrichment calculation

This approach was employed to compute the binding free energy of compds to attain a better estimation of binding powers/strengths and relative potencies for PIM-1K inhibitory activity (Sun *et al.*, 2014). The validation of virtual screening protocols was carried out by computing their enrichment factors as well as receiver operating curve (ROC) analysis (Hamza *et al.*, 2012; Sierra *et al.*, 2015).

ADME analysis

The compds were subjected for their ADME analysis to determine the drug-likeness properties by using QikProp module, version 4.3, Schrodinger, New York, 2015 (Becke, 1993; Lee *et al.*, 1988).

RESULTS AND DISCUSSION

Pharmacophore modeling

In 133 pharmacophore hypotheses of 62 variant, only 6 (AADRR.8, ADRRR.2, ADRRR.15, ADRRR.62, AARRR.2, and

AADRR.69) were selected (Table 2) for the development of the final QSAR model. These hypotheses include only three variants with different pharmacophoric features which display best alignment of actives representing top scoring hypotheses. Figure 1b–d shows the alignment of compd **25** (most active) with the highest scoring hypothesis (AADRR, ADRRR, and AARRR) from each of the three variants, respectively. The created hypotheses effectively recognized utmost significant pharmacophoric features suggested for the anticancer potential of 3-(pyrazin-2-yl)-1H-indazoles: A1 containing nitrogen atom, R for aromatic ring, and hydrogen bond donor (HBD) at D5. The deprivation of any of these structural features would compromise the anticancer potential.

3D-QSAR study

To develop a correlation among 3D spatial arrangement of the pharmacophoric features and anticancer activity of 3-(pyrazin-2-yl)-1H-indazoles (Table 3), the best 3D-QSAR model was created. Pharmacophore hypotheses were employed for the alignment of compds to build atom-based 3D-QSAR models through partial least square (PLS) method. The best generated 3D-QSAR model was based on the alignment of ADRRR.2 pharmacophoric features with the most active molecule (Fig. 2a). Table 4 shows the details of the best model of 3D-QSAR including three PLS factor model having excellent statistics as well as predictive capability as depicted from $r^2 = 0.922$, $q^2 = 0.8629$, and Pearson R = 0.9393 values. The model's validity was expressed by internal predictivity (q^2) which can be acquired by leave-one-out (LOO) method. The q^2 obtained through LOO method is statistically robust and more reliable as compared to r^2 as it is acquired by internal validation method. The high F value (78.8) designates a significant statistical regression model supported by small variance ratio ($p = 2.985e-011$), which denotes a high level of confidence. Smaller values of SD of regression (0.1929) and RMSE (0.214) provided an apparent suggestion that data which were used to create model in QSAR analysis are the best. A good correlation was obtained among estimated and actual anticancer activity (Table 1). The scatter plots between the estimated versus actual activities displayed that pIC_{50} values are efficiently speculated for training and test set molecules (Fig. 3a,b). The study results of 3D-QSAR can be seen in Figure 2b–d. Blue blocks present in the pharmacophore model (3D) denote the ligand regions in which particular structural attribute is essential for better activity, while red blocks refer that certain structural attributes are not important for activity. Here compd **25** is the most active inhibitor containing several substituents which affects various features, like HBD, electron-withdrawing, and hydrophobic effects. Introducing HBD and electron-withdrawing groups (EWGs) at ring (R17) lead to increased PIM-1K inhibition. The incorporation of EWGs on pyrazine ring causes decreased inhibition. The presence of hydrophobic groups showed different effects on various positions of these compds in which introduction on R17 is beneficial for activity, but on pyrazine ring the activity depends on *ortho*, *para,* and *meta* substitution.

Molecular docking studies

The active molecule **25** with receptor cavity is shown in Figure 4a. Here, indazole NH group was found engaged in hydrogen bond interaction with Glu121 in the hinge region. The Azaspiro group showed interaction with Asp186 and Glu171, essential for activity. The amine group of phenyl ring showed interaction with Asp131. The extra precision (XP) Gscore of compd **25** was −11.084. All these study data revealed the essential interactions for the ligand with the receptor for better PIM-1K inhibition. Another study for determining the PIM-1K and ligand interaction was established by carrying out molecular docking using the software Autodock Vina. The most active compd **25** binds with different sites on PIM-1K giving information for further structural optimization of active compds. The binding site (Fig. 4b) validates the previous study where different amino acid residues (AARs) like Lys67, Glu171, Glu121, and Asp128 were proven to be essential for activity (Asati *et al.*, 2018). The lowest value of RMSD 2.067 Å as well as binding affinity −9.4 kcal/mol proved better PIM-1K inhibitory activity. The hydrogen bond distance between Glu171, Glu121, and Asp128 to -NH were consecutively 3.3, 3.3, and 2.9 Å. When compd **1** docked with the PIM-1K, it showed only one interaction with Glu121 AAR (Fig. 4c). This interaction has 0.1 Å, the lowest RMSD value with −10.9 kcal/mol binding affinity evidenced least PIM-1K inhibitory activity. The top virtually hit compds, ZINC05885218, ZINC05888770, ZINC08652441, and ZINC73096248 exhibited best XP binding affinity with identical binding interactions to the receptor 2XJ1 evidenced by crystallographic ligand. These compds were showed similar binding attributes with the AARs Glu121, Lys67, Glu171, and Asp128 which are mandatory for PIM-1K inhibition. Three residues of PIM-1K, such as Glu124, Val126, and Ser54, adjacent to ATP-binding site also distinguished PIM-1K from PIM-2K. ZINC05885218 and ZINC05888770, and ZINC08652441 and ZINC73096248 displayed hydrogen bond interaction of -NH group with Glu121, important site for the PIM-1K inhibition (Fig. 5).

MM/GBSA-based rescoring

The Van der Waals (VDWs) interaction was present in docked compds between −33.06 and −54.86 kcal/mol. Similarly, Coulomb energy found in docked complexes fluctuated between positive and negative ranges, where ZINC73096248 showed −103.96 kcal/mol. The complex energy for all compds was found in the negative range between −11,335.46 and −11,403.11 kcal/mol, which evidently indicated that important interactions were VDWs forces. However, the best binding with ΔGbind was found at −55.02 kcal/mol for the top scored (XP docking) compd ZINC73096248 (−7.256 kcal/mol), which also exhibited higher Coulomb energy (−103.96 kcal/mol), and a slightly higher VDWs contribution (−35.76 kcal/mol) with complex energy (−11,368.68 kcal/mol). Henceforth, it is apparent that non-polar VDWs interactions are the principal driving force for binding the ligand in the PIM-1Ks catalytic pocket (Table 5).
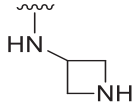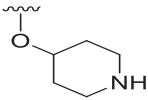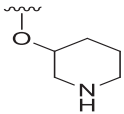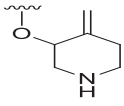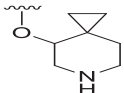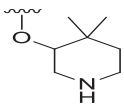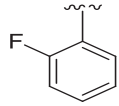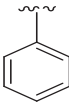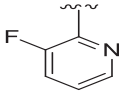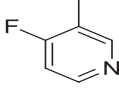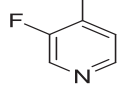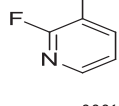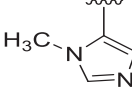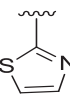
Estimation of the virtual screening efficiency

The present study finds the best protocol for the maximum active compd enrichment at the top 5% (6) of the given database. The retrieval of active compds incorporated into the decoy set is presented in Table 6. The actives exhibited enrichment factor with 0.97 ROC and 0.97 AUC.

Table 3. Anti-proliferative potentials of compds 1–29 against PIM-1K.
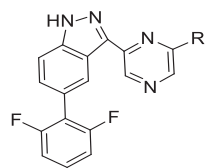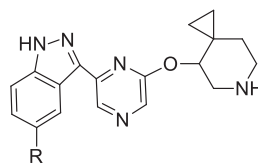
A (1–17) B (18–29)

Compd No.	R	Antiproliferative activity (IC$_{50}$, µM)	Antiproliferative activity (pIC$_{50}$, µM)
1		127	6.896
2		3	8.523
3		2	8.699
4		11	7.959
5		11	7.959
6		7	8.155
7		44	7.357
8		2	8.699
9		2	8.699
10		3	8.523

Continued

Compd No.	R	Antiproliferative activity (IC$_{50}$, µM)	Antiproliferative activity (pIC$_{50}$, µM)
11		15	7.824
12		8	8.097
13		7	8.155
14		3	8.523
15		0.4	9.398
16		3	8.523
17		0.9	9.046
18		1.6	8.796
19		4	8.398
20		2	8.699
21		4	8.398
22		3	8.523
23		15	7.824
24		3	8.523

Continued
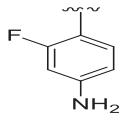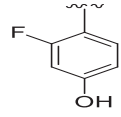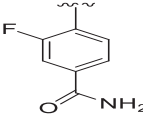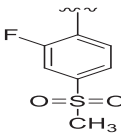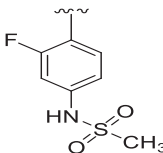
Compd No.	R	Antiproliferative activity (IC$_{50}$, µM)	Antiproliferative activity (pIC$_{50}$, µM)
25		0.2	9.699
26		0.4	9.398
27		0.5	9.301
28		1.4	8.854
29		0.3	9.523

Table 4. Statistical parameters of the best atom-based 3D-QSAR model generated by PHASE.

Hypothesis	PLS[a]	SD	r^{2}[b]	F[c]	P	Stability	RMSE	q^{2}[d]	Pearson-R
	1	0.4798	0.4687	19.4	0.0002239	0.9094	0.3518	0.6297	0.8104
	2	0.3346	0.7534	32.1	4.132e-007	0.6613	0.2748	0.7741	0.8899
ADRRR.2	3	0.1929	0.922	78.8	2.985e-011	0.3473	0.214	0.8629	0.9393
	4	0.144	0.9587	110.2	7.197e-013	0.3847	0.2387	0.8294	0.9144
	5	0.1059	0.9788	166.4	2.055e-014	0.3724	0.2586	0.7999	0.8972

[a]Factors in PLS regression model.
[b]r^2 value for the regression.
[c]Variance ratio.
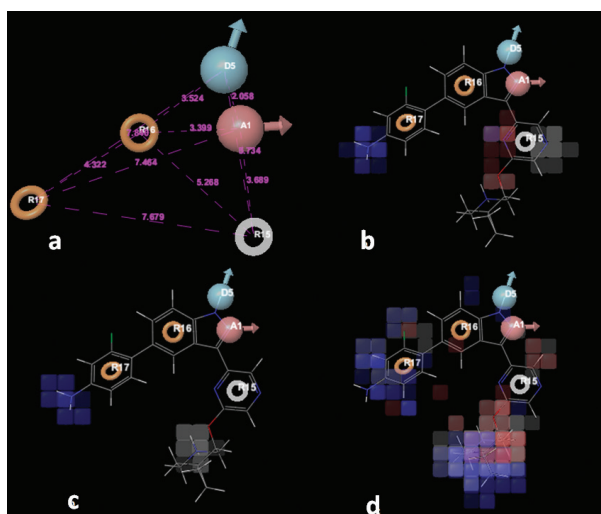[d]q^2 value for predicted activity of test set.

Figure 2. (a) Common pharmacophoric features of ADRRR.2; (b) the 3D-QSAR model (atom-based) for ADRRR.2; (c) HBD; and (d) hydrophobic effects.
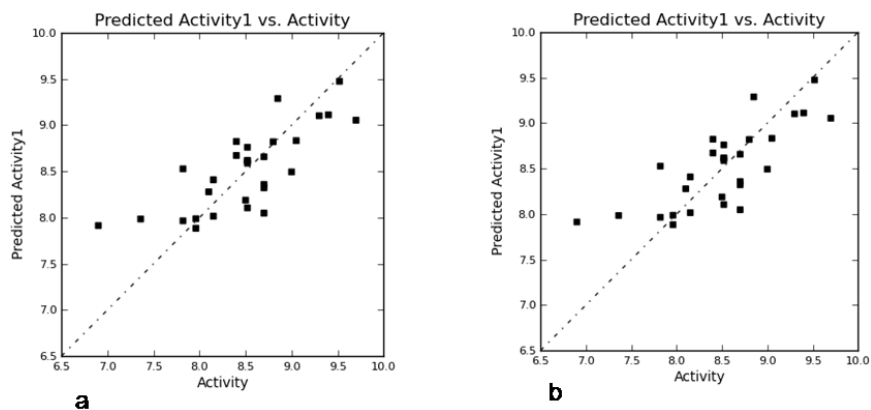
Figure 3. Scatter plots: (a) training set compd; (b) test set compd.
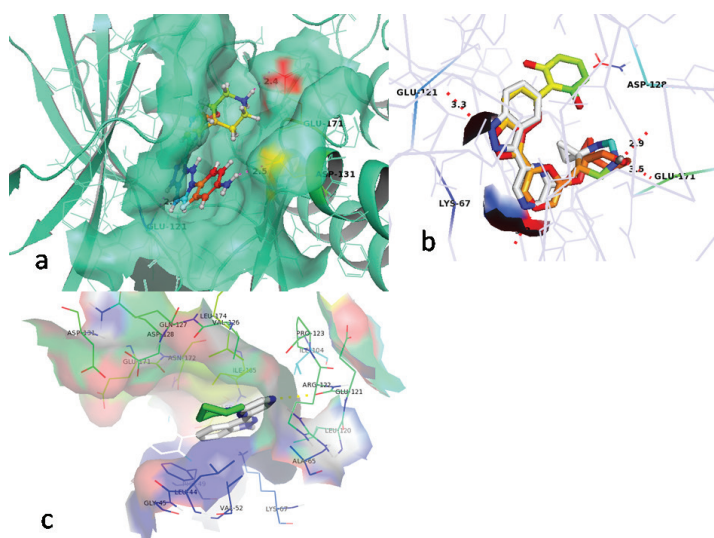
Figure 4. (a) Binding interaction of compd 25 with the active site of PIM-1K (PDB ID: 2XJ1); (b) comparison of binding interaction of the most active compd 25 and crystal ligand with receptor cavity of PIM-1K (PDB ID:2XJ1); and (c) binding interactions of the least active compd 1 with PIM-1K receptor cavity.

Figure 5. Hydrogen bond interaction (yellow dotted lines) of compds (red colour) ZINC05885218, ZINC05888770, ZINC08652441, and ZINC73096248, with AARs Asp186, Lys67, and Glu121 of PIM-1K (PDB ID: 2XJ1), respectively.

Table 5. Rescoring of virtually screened compds based on MM/GBSA.

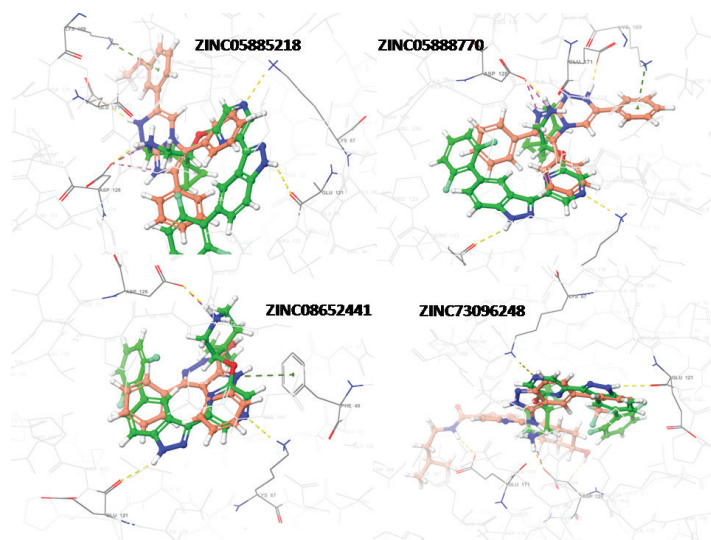| Compds	dG_Bind	dG_Bind_vdW	dG_Bind_Hbond	Ligand Strain Energy	Complex Energy	Ligand_ Energy	dG_Bind_Coulomb
ZINC05885218	−38.73	−54.86	−1.39	10.11	−11,403.11	-37.24	−17.69
ZINC05888770	−21.28	−33.06	−0.26	4.10	−11,335.46	12.95	70.03
ZINC08652441	−52.44	−34.24	−1.02	9.17	−11,361.29	18.29	−98.74
ZINC73096248	−55.02	−35.76	−1.55	9.88	−11,368.68	13.47	−103.96

Table 6. Enrichment factor calculation

Compds	Specificity	1-Specificity	Sensitivity	%Screen	%Actives Found
1	0.97	0.03	0.17	2.88	16.67
2	0.97	0.03	0.33	2.98	33.33
3	0.97	0.03	0.50	3.08	50.00
4	0.97	0.03	0.67	3.18	66.67
5	0.97	0.03	0.83	3.28	83.33
6	0.97	0.03	1.00	3.38	100.00

Table 7. Virtually screened compds (ADME and drug-likeness properties).

Compds	Mol_ MW	SASA[a]	HB donor	HB accpt	QPlogPo/w[b]	QPlogHERG[c]	QPPMDCK	QPPCaco[d]	QPlogKhsa[e]	Percent Human Oral Absorption[f]
ZINC05885218	380.45	673.84	2.00	4.25	4.94	−7.05	1,103.16	2,100.02	0.89	100.00
ZINC05888770	350.42	627.10	2.00	3.50	4.79	−6.95	1,128.08	2,143.89	0.85	100.00
ZINC08652441	261.28	486.19	2.00	3.50	2.36	−5.29	300.96	631.40	0.06	90.91
ZINC73096248	620.67	922.75	4.00	7.20	6.29	−7.01	282.74	284.41	1.36	81.77
1	379.47	633.01	3	5	2.853	−5.94	30.87	575.97	−0.05	74.02
2	273.22	433.54	1	3	2.364	−3.85	1,588.66	49.81	0.50	90.19
3	405.42	613.48	1	5	4.08	−5.72	1,223.0	690.69	0.59	100
4	440.46	690.84	3	6	4.02	−6.47	337.75	223.21	0.71	92.54
5	461.94	666.98	1	8	3.19	−5.82	102.15	152.06	0.48	84.68
6	303.37	522.46	3	5	1.17	−4.93	27.305	44.55	−0.01	63.32

[a]Total solvent accessible surface area (SASA) in Å^2 (range: 300–1,000).

[b]Predicted octanol/water partition coefficient (range: −2.0–6.5).

[c]Predicted blockage of hERG K+ channel (reasonable value <−8).

[d]Predicted Caco-2 cell permeability in nm/second.

[e]Prediction of human serum albumin binding (range: −1.5 – 1.5).

[f]Predicted human oral absorption on 0–100% scale.

ADME analysis

The study results showed that pharmaceutical and physicochemical characteristics of all investigated compds were within the acceptable range. The partition coefficient (QPlogPo/w) is a crucial factor for absorption estimation, ranging from 2.36 to 6.29, for the virtually screened compds. QPPCaco (cell permeability), a significant aspect for metabolism of drug, was found between the range of 284.41–2,143.89, and QPPMDCK ranged from 282.74 to 1,128.08. Generally, oral absorption percentage in humans for the screened compds was in the range of 81%–100%. The pharmacokinetic parameters for the screened compds were found within a permissible range (Table 7), thus interpreted as drug-like molecules.

CONCLUSION

The current study highlights the structural requirements of 3-(pyrazin-2-yl)-1H-indazole derivatives for the inhibitory activity against PIM-1K. The study results indicated that the incorporation of strong EWGs into pyrazine ring linked to indazole ring lead to a decreased PIM-1K inhibitory activity. Results of molecular docking of screened compds exhibited identical binding interactions within the PIM-1Ks catalytic pocket in comparison with their corresponding crystal structures. In conclusion, it is inferred that the acquired study results may serve as a guide for designing novel PIM-1K inhibitors, which could be an effective way to discover novel leads for the development of more active as well as safer anticancer agents/drugs.

CONFLICT OF INTEREST

The authors declared that they have no conflicts of interest.

REFERENCES

Asati V, Bharti SK. Design, synthesis and molecular modeling studies of novel thiazolidine-2,4-dione derivatives as potential anti-cancer agents. J Mol Struct, 2018; 1154:406–17.

Asati V, Mahapatra DK, Bharti SK. Thiazolidine-2,4-diones as multi-targeted scaffold in medicinal chemistry: potential anticancer agents. Eur J Med Chem, 2014; 87:814–33.

Becke AD. A new mixing of Hartree-Fock and local density-functional theories. J Chem Phys, 1993; 98:1372–7.

Brault L, Gasser C, Bracher F, Huber K, Knapp S, Schwaller J. PIM serine/threonine kinases in the pathogenesis and therapy of hematologic malignancies and solid cancers. Haematologica, 2010; 95(6):1004–15.

Cervantes-Gomez F, Lavergne B, Keating MJ, Wierda WG, Gandhi V. Combination of Pim kinase inhibitors and Bcl-2 antagonists in chronic lymphocytic leukemia cells. Leuk Lymphoma, 2016; 57(2):436–44.

Cortes J, Tamura K, DeAngelo DJ, Bono JD, Lorente D, Minden M, Uy GL, Kantarjian H, Chen LS, Gandhi V, Godin R, Keating K, McEachern K, Vishwanathan K, Pease JE, Dean E. Phase I studies of AZD1208, a proviral integration Moloney virus kinase inhibitor in solid and haematological cancers. Br J Cancer, 2018;118(11):1425–33.

Cuypers HT, Selten G, Quint W, Zijlstra M, Maandag ER, Boelens W, Wezenbeek PV, Melief C, Berns A. Murine leukemia virus-induced T-cell lymphomagenesis: integration of proviruses in a distinct chromosomal region. Cell, 1984; 37(1):141–50.

Dixon SL, Smondyrev AM, Knoll EH, Rao SN, Shaw DE, Friesner RA. PHASE: a new engine for pharmacophore perception, 3D QSAR model development, and 3D database screening: 1. Methodology and preliminary results. J Comput Aided Mol Des, 2006; 20(10–11):647–71.

Forshell LP, Li Y, Forshell TZP, Rudelius M, Nilsson L, Keller U, Nilsson J. The direct Myc target PIM3 cooperates with other PIM kinases in supporting viability of Myc-induced B-cell lymphomas. Oncotarget, 2011; 2(6):448–60.

Fox CJ, Hammerman PS, Cinalli RM, Master SR, Chodosh LA, Thompson CB. The serine/threonine kinase Pim-2 is a transcriptionally regulated apoptotic inhibitor. Genes Dev, 2003; 17(15):1841–54.

Friesner RA, Banks JL, Murphy RB, Halgren TA, Klicic JJ, Mainz DT, Repasky MP, Knoll EH, Shelley M, Perry JK, Shaw DE, Francis P, Shenkin PS. Glide: a new approach for rapid, accurate docking and scoring. 1. Method and assessment of docking accuracy. J Med Chem, 2004; 47(7):1739–49.

Friesner RA, Murphy RB, Repasky MP, Frye LL, Greenwood JR, Halgren TA, Sanschagrin PC, Mainz DT. Extra precision glide: docking and scoring incorporating a model of hydrophobic enclosure for protein-ligand complexes. J Med Chem, 2006; 49(21):6177–96.

Golbraikh A, Tropsha A. Predictive QSAR modeling based on diversity sampling of experimental datasets for the training and test set selection. J Comput Aided Mol Des, 2002; 16(5–6):357–69.

Halgren TA, Murphy RB, Friesner RA, Beard HS, Frye LL, Pollard WT, Banks JL. Glide: a new approach for rapid, accurate docking and scoring. 2. Enrichment factors in database screening. J Med Chem, 2004; 47(7):1750–9.

Hamza A, Wei NN, Zhan CG. Ligand-based virtual screening approach using a new scoring function. J Chem Inf Model, 2012; 52(4):963–74.

Irwin JJ, Shoichet BK. ZINC-a free database of commercially available compounds for virtual screening. J Chem Inf Model, 2005; 45(1):177–82.

Kamaria P, Kawathekar N. Ligand-based 3D-QSAR analysis and virtual screening in exploration of new scaffolds as plasmodium falciparum glutathione reductase inhibitors. Med Chem Res, 2014; 23:25–33.

Lather V, Kristam R, Saini JS, Kristam R, Karthikeyan NA, Balaji VN. QSAR models for prediction of glycogen synthase kinase-3b inhibitory activity of indirubin derivatives. QSAR Comb Sci, 2008; 27(6):718–28.

Lee C, Yang W, Parr RG. Development of the Colle-Salvetti correlation-energy formula into a functional of the electron density. Phys Rev B, 1988; 37(2):785–9.

Lipinski CA, Lombardo F, Dominy BW, Feeney PJ. Experimental and computational approaches to estimate solubility and permeability in drug discovery and development settings. Adv Drug Deliv Rev, 2001; 46(1–3):3–26.

Mikkers H, Nawijn M, Allen J, Brouwers C, Verhoeven E, Jonkers J, Berns A. Mice deficient for all PIM kinases display reduced body size and impaired responses to hematopoietic growth factors. Mol Cell Biol, 2004; 24(13):6104–15.

Nawijn MC, Alendar A, Berns A. For better or for worse: the role of pim oncogenes in tumorigenesis. Nat Rev Cancer, 2011; 11(1):23–34.

Sallam A, Houssen WE, Gissendanner CR, Orabi KY, Foudah AI, Sayed KE. Bioguided discovery and pharmacophore modeling of the mycotoxic indole diterpene alkaloids penitrems as breast cancer proliferation, migration, and invasion inhibitors. Medchemcomm, 2013; 4(10):1360–9.

Seeliger D, Groot BL. Ligand docking and binding site analysis with PyMOL and Autodock/Vina. J Comput Aided Mol Des, 2010; 24(5):417–22.

Shah UA, Deokar HS, Kadam SS, Kulkarni VM. Pharmacophore generation and atom-based 3D-QSAR of novel 2-(4-methylsulfonylphenyl) pyrimidines as COX-2 inhibitors. Mol Divers, 2010; 14(3):559–68.

Sierra C, Ordonez C, Saavedra A, Gallego JR. Element enrichment factor calculation using grain-size distribution and functional data regression. Chemosphere, 2015; 119:1192–9.

Sliwoski G, Kothiwale S, Meiler J, Lowe EW. Computational methods in drug discovery. Pharmacol Rev, 2014; 66(1):334–95.

Sun H, Li Y, Shen M, Tian S, Xu L, Pan P, Guan Y, Hou T. Assessing the performance of MM/PBSA and MM/GBSA methods. 5. Improved docking performance using high solute dielectric constant MM/GBSA and MM/PBSA rescoring. Phys Chem Chem Phys, 2014; 16(40):22035–45.

Tursynbay Y, Zhang J, Li Z, Tokay T, zhumadilov Z, Wu D, Xie Y. Pim-1 kinase as cancer drug target: an update. Biomed Rep, 2016; 4(2):140–6.

Wang HL, Cee VJ, Chavez FJ, Lanman BA, Reed AB, Wu B, Guerrero N, Lipford R, Sastri C, Winston J, Andrews KL, Huang X, Lee Mr, Mohr C, Xu Y, Zhou Y, Taskera AS. The discovery of novel 3-(pyrazin-2-yl)-1H-indazoles as potent pan-Pim kinase inhibitors. Bioorg Med Chem Lett, 2015; 25(4):834–40.

Watts KS, Dalal P, Murphy RB, Sherman W, Friesner RA, Shelley JC. ConfGen: a conformational search method for efficient generation of bioactive conformers. J Chem Inf Model, 2010; 50(4):534–46.

Xu Y, Brenning BG, Kultgen SG, Foulks JM, Clifford A, Lai S, Chan A, Merx S, McCullar MV, Kanner SB, Ho KK. Synthesis and biological evaluation of Pyrazolo[1,5-a]pyrimidine compounds as potent and selective Pim-1 inhibitors. ACS Med Chem Lett, 2014; 6(1):63–7.

Zhang Y, Wang Z, Li X, Magnuson NS. Pim kinase-dependent inhibition of c-Myc degradation. Oncogene, 2008; 27:4809–19.